A dynamic flux balance model and bottleneck identification of glucose, xylose, xylulose co-fermentation in Saccharomyces cerevisiae

Citation	Hohenschuh, W., Hector, R., & Murthy, G. S. (2015). A dynamic flux balance model and bottleneck identification of glucose, xylose, xylulose co-fermentation in Saccharomyces cerevisiae. Bioresource technology, 188, 153-160. doi:10.1016/j.biortech.2015.02.015
DOI	10.1016/j.biortech.2015.02.015
Publisher	Elsevier
Version	Version of Record
Terms of Use	http://cdss.library.oregonstate.edu/sa-termsofuse

Bioresource Technology 188 (2015) 153–160

Contents lists available at ScienceDirect

Bioresource Technology

journal homepage: www.elsevier.com/locate/biortech

A dynamic flux balance model and bottleneck identification of glucose, xylose, xylulose co-fermentation in *Saccharomyces cerevisiae*

William Hohenschuh [a], Ronald Hector [b], Ganti S. Murthy [a,*]

[a] Oregon State University, United States
[b] USDA, ARS, NCAUR, United States

HIGHLIGHTS

- Xylulose utilization limited by phosphorylation by xylulokinase in wt *S. cerevisiae*.
- Transport limits xylulose utilization in xylulokinase enhanced strains.
- HXT family of transporters responsible for xylulose transport in *S. cerevisiae*.
- Accounting for cell death produces improved modeling fit of batch fermentation.

GRAPHICAL ABSTRACT

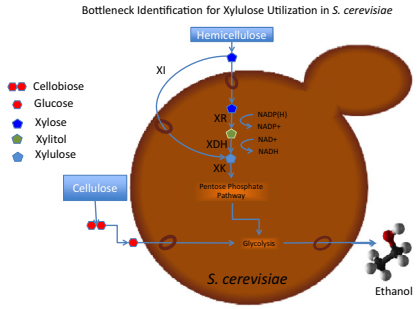

ARTICLE INFO

Article history:
Received 25 November 2014
Received in revised form 4 February 2015
Accepted 5 February 2015
Available online 20 February 2015

Keywords:
Xylose
Cellulosic ethanol
Fermentation
Pentose
Flux balance analysis

ABSTRACT

A combination of batch fermentations and genome scale flux balance analysis were used to identify and quantify the rate limiting reactions in the xylulose transport and utilization pathway. Xylulose phosphorylation by xylulokinase was identified as limiting in wild type *Saccharomyces cerevisiae*, but transport became limiting when xylulokinase was upregulated. Further experiments showed xylulose transport through the HXT family of non-specific glucose transporters. A genome scale flux balance model was developed which included an improved variable sugar uptake constraint controlled by HXT expression. Model predictions closely matched experimental xylulose utilization rates suggesting the combination of transport and xylulokinase constraints is sufficient to explain xylulose utilization limitation in *S. cerevisiae*.

1. Introduction

Lignocellulosic ethanol has the potential to displace the bulk of liquid fuels consumed in the US, but the adoption of biofuels will be driven more by economics than by the desire to decrease GHG emissions. Techno-economic analyses of lignocellulosic ethanol production have the cost of raw feedstocks to be one of the largest contributing factors to ethanol production cost (Sassner et al., 2008; Wingren et al., 2003). An efficient and complete conversion of feedstock sugars to ethanol is therefore required to make ethanol economically competitive with the production of conventional fossil transportation fuels.

Hexose sugars found in lignocellulosic biomass are readily fermentable by *Saccharomyces cerevisiae*, but the pentose sugar derived from hemicellulose is less readily fermentable. Successful fermentation of the hemicellulose sugars would increase ethanol yield by up to 40% and decrease production cost by upwards of 22% (Kumar et al., 2012). One method to capture this yield increase is to convert the main pentose sugar (xylose) to a more readily utilized form (xylulose) using an extracellular enzyme. Extracellular

* Corresponding author at: 116 Gilmore Hall, Corvallis, OR 97331, United States. Tel.: +1 541 737 6291.
E-mail address: MurthyG@ONID.OregonState.EDU (G.S. Murthy).

http://dx.doi.org/10.1016/j.biortech.2015.02.015
0960-8524/

xylulose can be utilized by *S. cerevisiae* with greater than 80% efficiency (Gong et al., 1981). Xylulose is taken up by wild-type *S. cerevisiae*, is converted to xylulose-5-phosphate by xylulokinase (XK), and is funneled through the pentose phosphate pathway to eventually produce ethanol. Utilization through this pathway is slow at approximately 1–2 orders of magnitude below *S. cerevisiae*'s glucose consumption rate (4 g/gDCW-h) (Sonnleitnert and Kappeli, 1986). Slow utilization increases production costs by requiring some combination of larger fermenters, longer fermentation periods, and increased yeast loading. Increasing the rate of utilization requires an understanding of possible enzymatic and transport bottlenecks. Previous work to expand an enzymatic bottleneck caused by constrained xylulokinase capacity yielded an increase in ethanol production rate from 0.04 to 0.23 grams per gram dry cell weight per hour (g/gDCW-h) (Lee et al., 2003). Other work aimed at increasing the capacity of downstream pentose phosphate pathway enzymes yielded an increase in utilization rate from 0.09 to 0.22 g/gDCW-h (Johansson and Hahn-Hägerdal, 2002; Matsushika et al., 2012).

The ability for enzymatic modifications to increase yield beyond 0.23 g/gDCW-h has not been demonstrated. This may be due to transport becoming the limiting reaction. Xylulose transport in *S. cerevisiae* is not well understood, but xylose transport has been more extensively studied (Hotta et al., 2009; Runquist et al., 2010; Sedlak and Ho, 2004; Tanino et al., 2010). *S. cerevisiae* does not have xylose specific transporters and xylose competes with hexose sugars for transport through hexose transporters. Xylulose transport may use similar transporters and transport mechanisms to its isomer xylose.

One attempt to model xylose transport focused on the transport of xylose through the native *S. cerevisiae* hexose transporter family (HXT family) (Bertilsson et al., 2007). Using a system of ODE's based on the known expression patterns and transport kinetics of the individual HXT transporters; the model was able to accurately represent the consumption of sugars in mixed xylose/glucose fermentation (Bertilsson et al., 2007). Assuming a similar transport pathway, the same technique could help to characterize the mechanism behind xylulose transport.

Flux balance analysis (FBA) is a type of constraint-based modeling that uses physical or chemical constraints to define all allowable sets of fluxes through a network. Constraint-based analysis assumes that the system is at steady state (i.e. that it is not accumulating metabolites and fluxes are constant) and that it is satisfying all physio-chemical constraints (reaction rates are within allowable ranges and metabolites used in all reactions are actually available). Flux balance analysis has been described at length in other works (Kauffman et al., 2003; Orth et al., 2010).

This work attempts to identify enzymatic and transport bottlenecks in the utilization of xylulose in *S. cerevisiae*. Using a flux balance approach in combination with Bertillson's sugar uptake approximation techniques the proposed bottlenecks are reconciled against the proposed mechanism of xylulose transport.

2. Methods

2.1. Fermentation experiments

2.1.1. Yeast strains

Strain names, genotypes, and descriptors are listed in Table 1. Five strains developed from the parent strain CEN.PK2-1C were utilized in this work. Included in these five strains were an empty vector control strain (referenced as wild type or YRH524), a strain containing a low copy plasmid encoding XK (referenced as low enhanced or YRH857), a strain with modified with a high copy plasmid encoding XK (referenced as high enhanced XK or YRH858), a wild type strain with HXT transporters 1–7 knocked out (referenced as Wild type HXT knockout or YRH1153), and a high copy XK enhanced HXT knockout strain (referenced as high copy HXT knockout or YRH1154).

To create strain YRH1087 lacking *HXT1* through *HXT7*, CEN.PK2-1C was transformed with PCR-generated DNA fragments that directed the replacement of the *HXT* genes with selectable markers. *HXT3*, *HXT6*, and *HXT7* were replaced with the *Kluyveromyces lactis URA3* gene. *HXT2* was replaced with the *K. lactis HIS5* gene. *HXT5*, *HXT1*, and *HXT4* were replaced with the *LEU2* gene. After each transformation, PCR products generated from the unique sequences created during the gene replacement confirmed that the genes were removed. The selectable makers used for the gene replacements were flanked by loxP sites and were subsequently removed by expression of Cre recombinase. After expression of Cre recombinase, several strains with uracil, histidine, and leucine auxotrophies were selected. Analysis of several of these strains by PCR using primers that flanked the markers further confirmed that the *HXT* genes were deleted and the markers removed. Strains YRH1153 and YRH1154 were generated by transforming YRH1087 with either pRS424 (empty vector) or pRH196 (XK expression vector).

A more detailed description of plasmids utilized in these strains can be found in Supplementary Table 1. Plasmid retention pressure was applied via a tryptophan selection marker that allowed only cells retaining the plasmid to grow on tryptophan lacking media.

2.1.2. Passage conditions

Yeast strains were propagated from stocks under sterile conditions. Colonies were grown on plates and transferred to 25 °C liquid passage media (6% glucose, 6.7 g/L YNB (without amino acids), 2 g/L amino acid dropout mix (lacking tryptophan), 1 mL/L Tween). Cultures were unstirred and were passaged every 2–4 days to maintain high cell density. Before experiments, cultures were harvested via centrifugation at 1000*g* for 10 min, the supernatant decanted, and the pellet re-suspended in deionized water.

2.1.3. Experimental conditions

Batch fermentations were carried out in 25 °C water baths. Media composition was similar to that of passage media with the

Table 1
Description of strains.

Strain definitions		
Strain	Descriptor	Genotype
CEN.PK2-1C	Parent strain	*MATa ura3-52 trp1-289 leu2-3_112 his3Δ1 MAL2-8c SUC2*
YRH524	Wild type control	CEN.PK2-1C + pRS414 (empty TRP1-marked vector)
YRH857	Low enhanced XK	CEN.PK2-1C + pRH195 (low-copy vector + *XKS1*)
YRH858	High enhanced XK	CEN.PK2-1C + pRH196 (high-copy vector + XKS1)
YRH1087	HXT knockout	CEN.PK2-1C *hxt1Δ*, *hxt2Δ*, *hxt3Δ*, *hxt4Δ*, *hxt5Δ*, *hxt6Δ*, *hxt7Δ*
YRH1153	Wild type control HXT knockout	CEN.PK2-1C *hxt1Δ*, *hxt2Δ*, *hxt3Δ*, *hxt4Δ*, *hxt5Δ*, *hxt6Δ*, *hxt7Δ* + pRS424
YRH1154	High enhanced XK HXT knockout	CEN.PK2-1C *hxt1Δ*, *hxt2Δ*, *hxt3Δ*, *hxt4Δ*, *hxt5Δ*, *hxt6Δ*, *hxt7Δ* + pRH196

Table 2
Initial conditions for each of seven validation experiments.

Experiment	Initial glucose (g/l)	Initial xylose (g/l)	Initial xylulose (g/l)	Initial biomass (g/l)	Strains
E1*	22.77 ± 1.89	24.78 ± 1.35	11.11 ± 0.54	11.20 ± 0.31	Wild type XK,
E2	0.00 ± 0.00	37.51 ± 0.98	20.20 ± 0.52	17.92 ± 0.54	Low enhanced XK,
E3	0.82 ± 0.16	102.85 ± 7.35	37.24 ± 6.15	19.58 ± 1.60	High enhanced XK
E4	0.00 ± 0.00	43.47 ± 1.17	60.68 ± 1.18	9.89 ± 1.35	
E5	0.00 ± 0.00	33.45 ± 0.54	71.11 ± 0.97	17.17 ± 0.49	
E6	0.08 ± 0.32	77.27 ± 3.41	101.29 ± 8.97	11.26 ± 1.31	Wild type XK,
E7*	32.59 ± 1.49	34.84 ± 1.27	53.67 ± 3.47	9.88 ± 0.35	Low enhanced XK,
E8**	33.09 ± 2.20	29.40 ± 0.59	15.77 ± 10.75	10.86 ± 0.42	High enhanced XK, Wild type XK HXT-, High enhanced XK HXT-

* Denotes experiments from which fitting data was drawn.
** E8 is an extension of experiment of E7 (after the initial 48 h E8 replicates were spiked with glucose syrup to produce the starting conditions listed. Different xylulose consumption rates left different xylulose concentrations for different strains producing the xylulose high standard deviation).

exception of the carbon source. Different ratios and concentrations of glucose, xylose, and xylulose were used in each experiment in an attempt to saturate the xylulose utilization of the cells. Measured initial concentrations for each experiment is shown in Table 2. In general glucose concentrations ranged from 0 to 35 g/L, xylose from 25 to 100 g/L, and xylulose from 5 to 100 g/L.

2.1.4. Data collection

Cell density was monitored through offline spectrophotometric absorbance measurements at 660 nm. Media composition was monitored through offline HPLC measurements. HPLC separation was performed on a BioRad HPX-87H column maintained at 65 °C with a 0.01 N H_2SO_4 mobile phase and a 0.6 mL/min flow rate. Relevant compounds (glucose, xylose, xylulose, acetic acid, lactic acid, succinic acid, glycerol, and ethanol) were quantified via a refractive index detector.

2.2. Flux balance analysis

2.2.1. Basic model structure

This model is based on the previously developed genome scale model iMM904. This model is built into a custom dFBA (dynamic flux balance analysis) loop that integrates fluxes over 30 s time steps (Fig. 1). This technique is similar to that used by Mahadevan et al. (2002) (Mahadevan et al., 2002). In this technique, a vector z contains the media metabolite concentrations in moles. The rate of change of each component in z is related to the stoichiometric matrix of the metabolic matrix A (stoichiometry is also in mol units), the rate of each metabolic flux contained in the vector v in units of moles per hour, and the current biomass concentration X in grams per liter (Eq. (1)). In turn, biomass is created according to the growth rate μ, determined as the weighted sum of the reactions that synthesize growth precursors w_i.

$$\frac{dz}{dt} = AvX, \quad \frac{dX}{dt} = \mu X, \quad \mu = \sum w_i v_i \tag{1}$$

At each iteration of the dFBA the composition of the media is used to calculate new flux bounds for sugar uptake (see Section 2.2.2), a linear solver is used to identify optimal flux rates through the cell, and the media composition is updated to reflect the effects of the optimal flux into and out of the cell. This loop repeats until the designated run length is completed.

2.2.2. Sugar transport model

The sugar transport model developed for xylulose was based on a transport model described originally for xylose transport (Bertilsson et al., 2007). This model assumes all sugar transport to be facilitated by the HXT family of glucose transport proteins. It derives the expression of individual transporters based on glucose

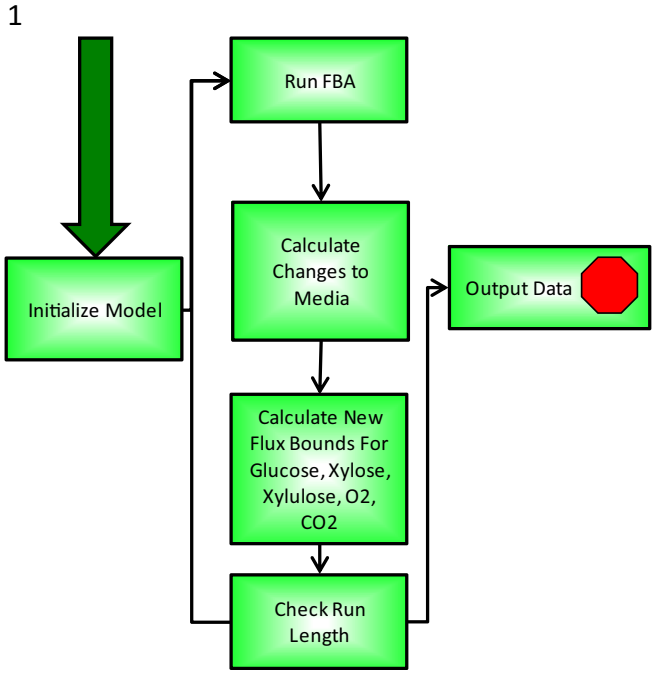

Fig. 1. Basic dFBA looping structure – an FBA is used to calculate an optimal flux distribution. This flux is extrapolated over a 30 s time step and results in changes to the media composition. The composition of the media dictates new allowable flux bounds that are used as new constraints for the next FBA iteration.

concentration in the media (Fig. 2a) (Diderich, 1999; Liang and Gaber, 1996; Ozcan and Johnston, 1995). This relative expression is expressed as θ_{HXTi} in model Eqs. (2.1) and (2.2). The sugar uptake through each transporter (scaled by the relative expression) was described for both xylose (xyl) and glucose (glu) with Michaelis–Menten kinetics (Eqs. (2.1) and (2.2)). The total transport was equal to the sum of transport through each transporter (Eqs. (2.3) and (2.4)). The model developed in this work includes an additional set of corresponding equations for xylulose (xylu) uptake and incorporates xylulose competitive inhibition into Eqs. (2.1) and (2.2).

$$v_{HXT1,glu} = \theta_{HXT1} \times \frac{v_{\max HXT1,glu} \times S_{glu}}{K_{m,HXT1,glu} \times \left(1 + \frac{S_{xyl}}{K_{m,HXT1,xyl}}\right) + S_{glu}} \tag{2.1}$$

$$v_{HXT1,xyl} = \theta_{HXT1} \times \frac{v_{\max HXT1,xyl} \times S_{xyl}}{K_{m,HXT1,xyl} \times \left(1 + \frac{S_{glu}}{K_{m,HXT1,glu}}\right) + S_{xyl}} \tag{2.2}$$

$$r_{glu} = v_{HXT1,glu} + v_{HXT2,glu} + v_{HXT3,glu} + v_{HXT4,glu} + v_{HXT6/7,glu} \quad (2.3)$$

$$r_{xyl} = v_{HXT1,xyl} + v_{HXT2,xyl} + v_{HXT3,xyl} + v_{HXT4,xyl} + v_{HXT6/7,xyl} \quad (2.4)$$

$$\text{if } r_{glu} + r_{xyl} > r_{\max,glu,flux}, \quad \text{then } \alpha = \frac{r_{\max,glu,flux}}{r_{glu} + r_{xyl}} \quad (2.5)$$

$$\text{if } r_{glu} + r_{xyl} \leqslant r_{\max,glu,flux}, \quad \text{then } \alpha = 1 \quad (2.6)$$

where $v_{HXTi,glu}$ = rate of glucose transport HXT transporter i (g/gDCW-h), θ_{HXTi} = relative expression of HXT transporter i (unitless scalar), S_{glu} = media concentration of glucose (g/l), r_{glu} = sum of glucose transport through HXT transporters (g/gDCW-h), α = scalar (unitless scalar).

The transport model deviates from Bertilsson's model in how it imposes a total sugar flux constraint. In Bertilsson's model, if the sum of calculated sugar fluxes exceeded 4 g/gDCW-h they were scaled proportionally to be within the 4 g/gDCW-h limit while maintaining the ratio of glucose to xylose transport (Eqs. (2.5) and (2.6)). The model in this work seeks to more realistically constrain sugar flux by fitting each maximal sugar flux (in the absence of other sugars) separately and defining the total transport capacity of the transporter set in terms of all transported sugars.

For example, using the a maximal flux rate of 4 g/gDCW-h for glucose and (a hypothetical) 2 g/gDCW-h for xylose, and assuming a uniform transportation rate, the time to transport 1 g/g-DCW glucose would be 15 min while transporting 1 g/gDCW-h of xylose would take 30 min. Therefore the capacity is four units of glucose per hour, or two units of xylose, or some combination of glucose and xylose the sum of which does not violate the transport capacity. It follows that one xylose and two glucose would be acceptable as the total transport capacity is not violated (60 total minutes required), but that three glucose and one xylose would be unacceptable as the total transport capacity is violated (105 total minutes required) even while individual transport capacities are within allowable ranges (Fig. 2b). The maximum level of xylulose transport is not well defined for all conditions. As a result the "time scalar" for xylulose was fit as a model parameter.

2.2.3. Alternative sugar transporters

To account for the possibility of non-HXT transporters acting on xylulose an additional transporter was added to the model. This transporter represented the aggregate xylulose transport through all non-HXT transporters. The fitting of this transporter is discussed in Section 3.2.1, but in terms of model development it is of constant expression level and is included in the summed transport levels when calculating the sugar time scalar.

2.2.4. End dynamics of batch fermentation

The model developed here was designed to predict the outcome of a series of batch fermentation experiments. During initial model development it was assumed that all sugar would be consumed. However, experimental data showed that in many cases sugar consumption arrested well before exhaustion. This rarely happens in glucose fermentation in complex media with adequate micronutrients and when ethanol is low (below 100 g/l), but because of the low efficiency with which xylulose is taken up, it was hypothesized that cells may have difficulty reaching the minimum ATP production required for maintenance and that this may have led to cell death. A standard dynamic FBA has no way of modeling this because the required ATP maintenance is a fixed constraint.

In an attempt to better model reality a cell death equation was added to the model. When this reaction was active it decreased viable biomass and returned a percentage the metabolites required for cell growth to the surviving cells. This recycling of nutrients allowed a portion of the cells to produce the minimum ATP required for maintenance, survive, and continue to slowly consume xylulose. After several iterations of cell death, this surviving fraction would be sufficiently small to halt fermentation.

3. Results and discussion

3.1. Fermentation results

A major objective of the batch experiments was to identify the bottleneck in xylulose utilization. It had been hypothesized that this bottleneck would either be in the transport of xylulose into the cell or in the conversion of xylulose to xylulose-5-phosphate.

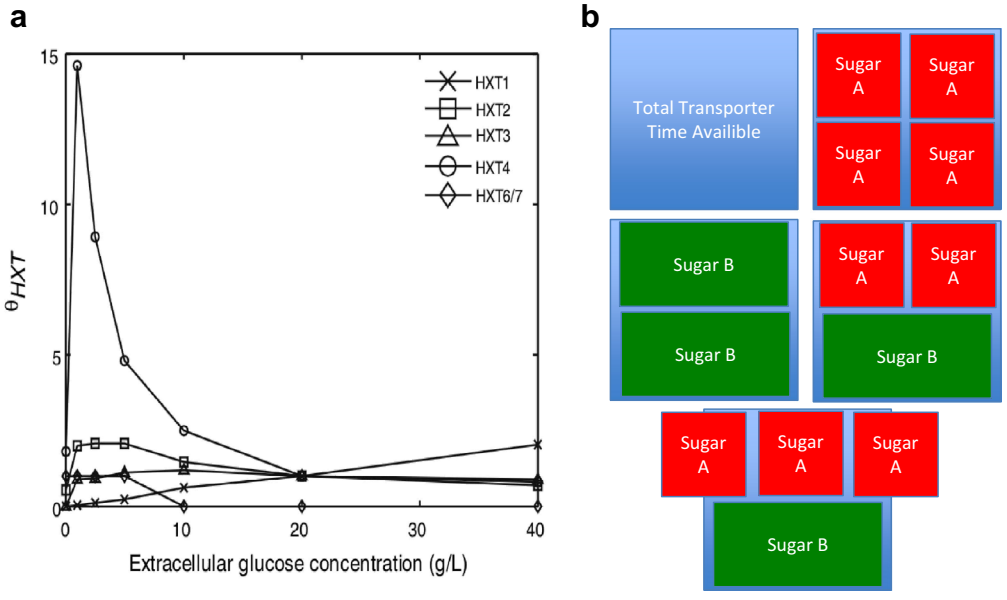

Fig. 2. (a) HXT expression level correlation with glucose – these correlations were used in Bertilsson's model and are used here. (b) Rational for a sugar time scalar – unlike Bertilsson's model that used the same scalar for all sugars, this model considers the unique maximum transport rate for each sugar to calculate the scalar.

To test this hypothesis experimental results from the wild type, low copy XK, and high copy XK strains were compared. These strains are genetically identical except in the level of XK expression. If, for a given experiment, strains with higher XK capacity showed an increased rate of xylulose utilization it would be concluded that XK was the limiting reaction in the utilization of xylulose. Conversely, if the rates of xylulose utilization (for a single experiment) were the same amongst these strains independent of XK capacity, it would be concluded that XK was not the limiting reaction.

In comparing wild-type (YRH524) *S. cerevisiae* to strains with excess of XK (with high or low copy XK plasmid), the wild-type strain showed a decreased average xylulose utilization rate over the first 12 h of fermentation in four of seven independent experiments. Under experimental treatments E1, E2, E3, and E4 there was a statistically relevant difference (p-value < 0.05) between the wild-type strain (YRH524) and each of the XK enhanced strains. Experimental condition E3 showed average consumption rates slightly higher in all XK enhanced strains, but the differences were not large enough to be statistically valid (p-value 0.096).

With three of four experimental treatments showing a significantly decreased utilization rate in YRH524 and one additional experiment showing small but statistically insignificant support for this trend (Fig. 3b), this data as a whole supports the hypothesis that XK was limiting in strain YRH524. Additionally, the lack of statistically significant difference between the low and high enhanced strains suggests that XK is not limiting in these strains.

Xylulose transport was another proposed xylulose utilization bottleneck. The HXT family of proteins was previously shown to be active in xylose transport and was hypothesized to be also active in xylulose transport. The expression pattern of the HXT family of proteins is well correlated with the presence of glucose, but the quantity of sugar transported also depended on the concentration of available sugars competing for transporters. In an attempt to understand the kinetics of xylulose transport an attempted was made to saturate xylulose transport when glucose concentration was near zero.

It was expected that xylulose transport would increase according to standard Michaelis–Menten kinetics and eventually saturate. However, when xylulose concentration was compared to xylulose consumption rate, no clear pattern emerged (Fig. 3a). In each experimental case xylulose consumption rate peaked at between 0.26 and 0.18 g/gDCW-h. This suggests that xylulose saturates its transporters at relatively low concentration, but it does not explain why each experiment had a different transport rate at the same low sugar concentration. For example E1 reached 0.18 g/gDCW-h or transport at 15 g/L xylulose, but E6 was only able achieve the same rate of transport at greater than 50 g/l xylulose.

When the same consumption data was plotted against time the consumption rate between experiments appears to be much more consistent. It was noted that the strains used in the experiments were cultured on a glucose media and that the start of each experiment (or in the first few hours for condition E1 in which glucose was present) would correspond to when glucose was exhausted. While the expression of the HXT family of transporters was known, these measurements were taken at near steady state conditions. The rate of change between expression states was therefore not determined. Since the strains used in the experiments were cultured on glucose prior to the experiments, time zero (or shortly thereafter for E1 for which the experimental media contained glucose) was when glucose levels would drop from high to low triggering a change in expression pattern. This change may happen over a predictable timeline resulting in the consistent consumption pattern in Fig. 3c. This sort of pattern would be indicative of a transporter expressed under glucose conditions similar to the HXT family of proteins.

To confirm the action of the HXT family of proteins in xylulose transport, a HXT knockout strain that was genetically identical to the High Enhanced XK strain except that it was deficient in HXT transporters 1–7 was utilized. In two of three experiments utilizing this strain there was a statistically significant decrease in xylulose consumption compared to the non-knockout strain. In the third experiment there was a non-statistically significant difference supporting the same trend (p-value = 0.067) (Fig. 3d). This suggests that the HXT family of proteins is active in xylulose transport, but because the knockout still displayed xylulose transport, the HXT family of proteins is not sufficient to explain all xylulose transport. This could be due to up regulated tertiary transporters discussed further in Section 3.2.

3.2. Modeling results

3.2.1. Model fitting

Model parameters (Table 3) were fit in three steps. First, the bounds for the aggregate transporter (accounting for previously unexplained transport of glucose and xylulose in HXT negative strains) were set directly from the observed correlation between transport in HXT negative strains and available glucose. Second, the parameters common to all strains (dv/dt for HXT transport change, xylose size scalar, xylulose scalar, ATP maintenance, death reaction recovery percent) were set using a particle swarm heuristic. This heuristic sought to minimize the objective function described in Eq. (3). The objective function considered glucose, xylose, xylulose, glycerol, acetic acid, lactic acid, and succinic acid concentration in the media at each sample time throughout two experiments with different ratios of glucose, xylose, and xylulose. This stage of fitting was based on the strain with the highest XK capacity as experimental data suggested that XK was not limiting in this strain.

$$\text{Objective} = \sum_{n=7} |\text{Experimental measurement} - \text{model prediction}| \tag{3}$$

Finally, since multiple strains were modeled with differing xylulokinase expression levels and reaction capacities, the upper bounds for XK were fit for each strain. In all but the most XK limited strain the model fit does not improve with constraining XK capacity. For these strains the XK capacity was unconstrained at 1000 mM/gDCW-h.

The fitting of xylulokinase capacity provided support for the experimental finding that XK was limiting in the wild type strain, but not in XK enhanced strains. In the wild type strain, the value of the objective value decreased (became better) as XK capacity was incrementally constrained (Fig. 4a). This suggests that constraint removed unrealistically high capacity before finding an optimal (maximum realizable) XK capacity and finally becoming over constrained causing the objective value to become worse. Constraint did not improve the objective value for either the low-enhanced XK strain (Fig. 4b) or the high-enhanced XK strain (data not shown). This is expected as experimental data suggested XK was not limiting in these strains.

3.2.2. Model validation

This model was fit using a single run from each of two experiments. To validate the model a larger experimental data set was created consisting of seven total experiments. The initial conditions averaged across all strains and replicates (minimum 3) for these experiments are listed in Table 2. Validation runs compared

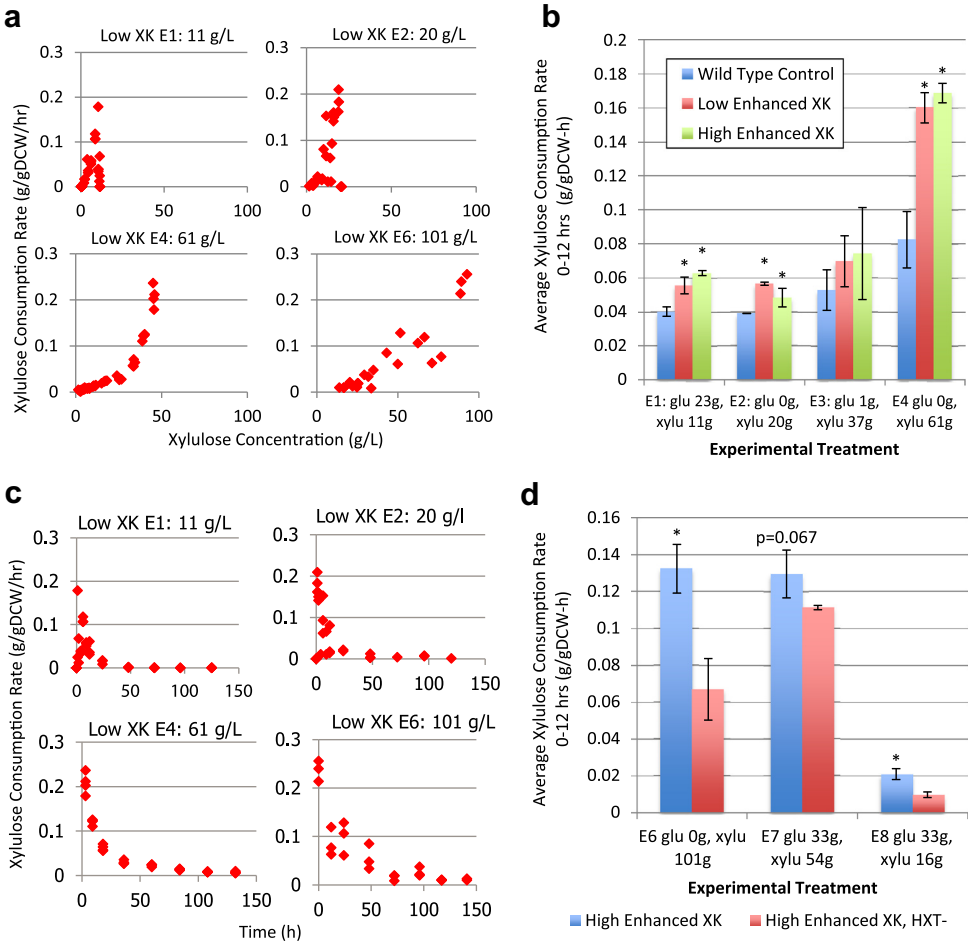

Fig. 3. (a) Xylulose consumption rate in a low-enhanced XK strain plotted as a function of xylulose concentration. (b) Xylulose consumption rate comparison between wild type, low-enhanced XK, and high-enhanced XK in 4 independent experiments. *Denotes a statistically significant difference to wild type strain. Error bars are the standard deviation of three replicates. (c) Xylulose concentration rate in a low-enhanced XK strain plotted as a function of experiment time progression. (d) Comparison of xylulose utilization rate over the initial 12 h of fermentation in a high-enhanced XK strain and a high-enhanced XK HXT-strain.

the measured sugar consumption averaged across all replicates for a given strain at each sample point in an experiment. The three main goals of validation were to (1) verify that the HXT model of sugar uptake was sufficient to explain sugar uptake, (2) show that incorporation of the cell death into the model results in a better model fit to experimentally observed sugar uptake profiles, and (3) consider the accuracy of the model in predicting the production of secondary metabolites.

Overall, modeled xylulose uptake rates during the initial fermentation (before cell death played a large role) closely approximated those observed during batch experiments. The internal dynamics of xylulose consumption were not strictly constrained (except in the wild type XK where XK capacity was constrained in the model). This suggests that the constraint of the xylulose transport pathway was sufficient to approximate xylulose utilization. This points to xylulose transport as the bottleneck for the XK enhanced strains.

The low and high-enhanced strains exhibited strong correlation between the model and experimental data in terms of sugar uptake (Fig. 5b, c, e, f, h and i). The wild type strain performed

Table 3
Best parameter fits – this table lists parameters, their description, and the best-identified fit using the Monte Carlo method described above. These values were used in modeling throughout the rest of this work.

Parameter fits used in modeling		
Parameter	Description	Value
XK capacity	Maximum capacity of xylulokinase (strain wt XK strains, all other strains)	0.4376, 1000 mM/gDCW-h
Theta max growth ratio	The maximum scalar by which the sugar consumption rate could increase in one time step	1.2932
Theta max degradation ratio	The minimum scalar by which the sugar consumption rate could decrease in one time step	0.935
Xylulose time scalar	The time scalar used to compare xylulose and glucose for transport	600.0975
Xylose time scalar*	The time scalar used to compare xylose and glucose for transport	55.556
Death recovery percentage	The percentage of cell metabolites recovered by living cell population after cell death	66.391%
ATP maintenance	The ATP cost to maintain a cell	0.988819 mM/gDCW-h

* Since xylose consumption was not possible in the model this parameter.

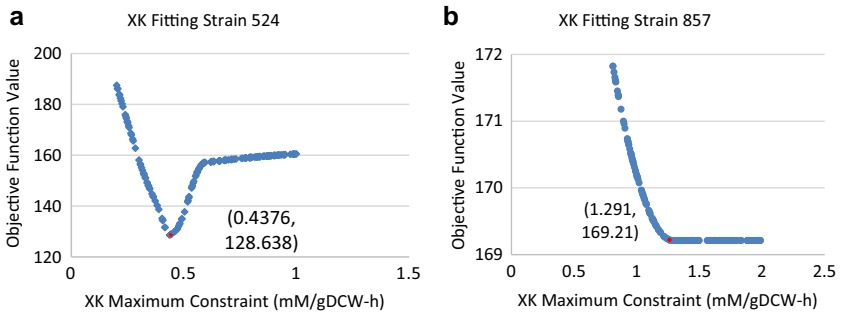

Fig. 4. Fitting of XK maximum rate constraint in a wild type control strain (a) and a low-enhanced XK strain (b). In these figures a lower objective function value is more optimal. Data label represents the best-identified fit.

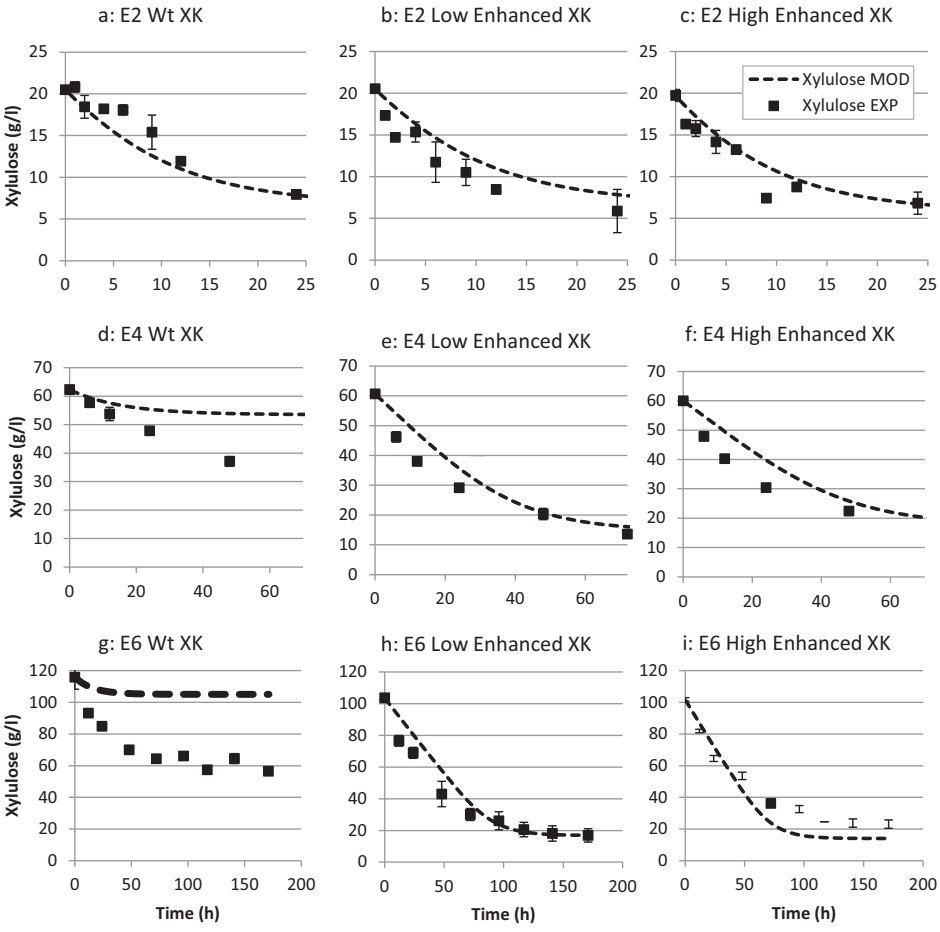

Fig. 5. Modeled and experimental xylulose concentration over time for three experimental conditions (E2, E4, and E6) – low and high XK enhanced strains fit well, but wild type XK strain terminates xylulose consumption prematurely suggesting that its XK capacity has been somewhat over constrained. Markers represent experimental data. Dashed line represents model data. Error bars are the standard deviation of three replicates.

well at lower sugar concentration, but was the poorest fitting for sugar concentrations above 50 g/l (Fig. 5e, f, h and i). For this strain the model predicted premature stoppage for sugar consumption. This trend was exacerbated at high sugar concentration and suggests that XK may have been over constrained or that the required sugar uptake for ATP maintenance was set too high.

The end dynamics of batch fermentation captured more accurately through the implementation of a death parameter in the flux balance model (Fig. 6a). Without this parameter, modeled runs would either consume all available sugar (when ATP maintenance was set very low) or would consume until ATP maintenance could not be satisfied resulting in a model error.

The ability of the death parameter to capture experimental results is highly sensitive to the value of the ATP maintenance parameter which is set as a constant in this model. However ATP maintenance levels for a single organism have been shown to change in correlation with media composition (Olz et al., 1993). Due to this limitation, the model tends to terminate sugar consumption prematurely. This trend is especially apparent in experimental treatments with low starting xylulose concentrations (Fig. 6b). This suggests that the level of sugar required to satisfy ATP maintenance may be lower for low sugar concentration (and thus low ethanol producing indicating lower ethanol stress) experimental conditions and that the death parameter requires greater study. Further, actual cell viability was not measured

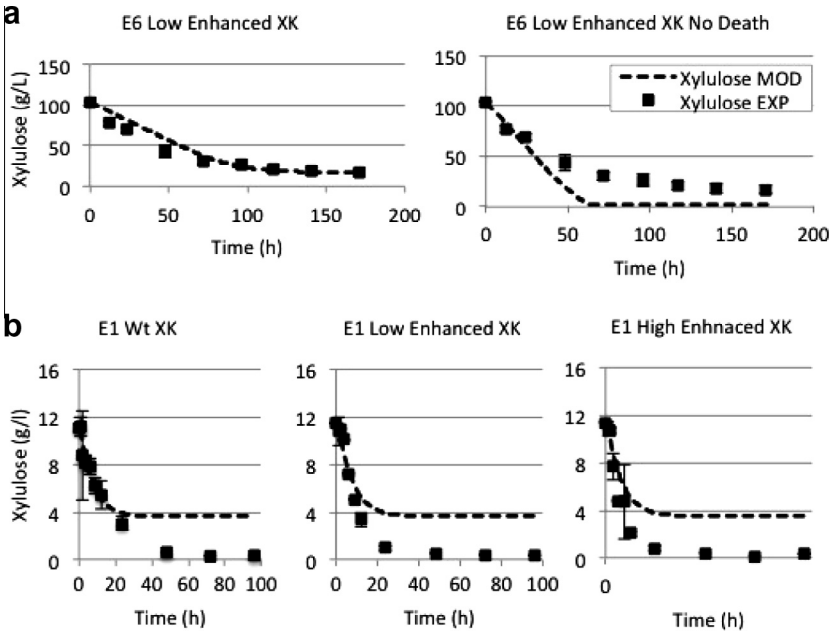

Fig. 6. (a) Comparison of model fit with and without cell death function – including cell death allows for incomplete xylulose consumption. (b) Cell death function fit at with low starting xylulose – with low starting sugar all strains consume sugar to below detectable levels. This suggests that a lower requirement for ATP maintenance would be more appropriate for modeling low sugar (and subsequently low ethanol) experiments. Markers represent experimental data. Dashed line represents model data. Error bars are the standard deviation of three replicates.

experimentally. Therefore, while the death parameter improves the data fit, the mechanism is not confirmed.

4. Conclusion

The model developed in this work demonstrates that HXT transport limitation and xylulokinase capacity constraint are sufficient to explain sugar transport during mixed sugar fermentation in *S. cerevisiae*. The inclusion of a cell death and metabolite recycle within the model allows for a better representation of end dynamics of batch fermentations. The predictive capabilities of the model allow for the validation of xylulose utilization bottlenecks identified in the experimental work and should allow for more directed modification of *S. cerevisiae* in the future.

Appendix A. Supplementary data

Supplementary data associated with this article can be found, in the online version, at http://dx.doi.org/10.1016/j.biortech.2015.02.015.

References

Bertilsson, M., Andersson, J., Lidén, G., 2007. Modeling simultaneous glucose and xylose uptake in *Saccharomyces cerevisiae* from kinetics and gene expression of sugar transporters. Bioprocess Biosyst. Eng. 31, 369–377. http://dx.doi.org/10.1007/s00449-007-0169-1.

Diderich, J.A., 1999. Glucose uptake kinetics and transcription of HXT genes in chemostat cultures of *Saccharomyces cerevisiae*. J. Biol. Chem. 274, 15350–15359. http://dx.doi.org/10.1074/jbc.274.22.15350.

Gong, C.-S., Chen, L.-F., Flickinger, M.C., Chiang, L.-C., Tsao, G.T., 1981. Production of ethanol from D-xylose by using D-xylose isomerase and yeasts. Appl. Environ. Microbiol. 41, 430–436.

Hotta, A., Tanino, T., Ito, T., Hasunuma, T., Ogino, C., Kondo, A., Ohmura, N., 2009. Bioethanol production from mixed sugars using sugar uptake ability enhanced yeast strain by overexpression of transporters. J. Biosci. Bioeng. 108, S53. http://dx.doi.org/10.1016/j.jbiosc.2009.08.152.

Johansson, B., Hahn-Hägerdal, B., 2002. The non-oxidative pentose phosphate pathway controls the fermentation rate of xylulose but not of xylose in *Saccharomyces cerevisiae* TMB3001. FEMS Yeast Res. 2, 277–282.

Kauffman, K.J., Prakash, P., Edwards, J.S., 2003. Advances in flux balance analysis. Curr. Opin. Biotechnol. 14, 491–496. http://dx.doi.org/10.1016/j.copbio.2003.08.001.

Kumar, D., Juneja, A., Hohenschuh, W., Williams, J.D., Murthy, G.S., 2012. Chemical composition and bioethanol potential of different plant species found in Pacific Northwest conservation buffers. J. Renew. Sust. Energy 4, 063114. http://dx.doi.org/10.1063/1.4766889.

Lee, T.-H., Kim, M.-D., Park, Y.-C., Bae, S.-M., Ryu, Y.-W., Seo, J.-H., 2003. Effects of xylulokinase activity on ethanol production from D-xylulose by recombinant *Saccharomyces cerevisiae*. J. Appl. Microbiol. 95, 847–852. http://dx.doi.org/10.1046/j.1365-2672.2003.02055.x.

Liang, H., Gaber, R.F., 1996. A novel signal transduction pathway in *Saccharomyces cerevisiae* defined by Snf3-regulated expression of HXT6. Mol. Biol. Cell 7, 1953.

Mahadevan, R., Edwards, J.S., Doyle, F.J., 2002. Dynamic flux balance analysis of diauxic growth in *Escherichia coli*. Biophys. J. 83, 1331.

Matsushika, A., Goshima, T., Fujii, T., Inoue, H., Sawayama, S., Yano, S., 2012. Characterization of non-oxidative transaldolase and transketolase enzymes in the pentose phosphate pathway with regard to xylose utilization by recombinant *Saccharomyces cerevisiae*. Enzyme Microb. Technol. 51, 16–25. http://dx.doi.org/10.1016/j.enzmictec.2012.03.008.

Olz, R., Larsson, K., Adler, L., Gustafsson, L., 1993. Energy flux and osmoregulation of *Saccharomyces cerevisiae* grown in chemostats under NaCl stress. J. Bacteriol. 175, 2205–2213.

Orth, J.D., Thiele, I., Palsson, B.Ø., 2010. What is flux balance analysis? Nat. Biotechnol. 28, 245–248.

Ozcan, S., Johnston, M., 1995. Three different regulatory mechanisms enable yeast hexose transporter (HXT) genes to be induced by different levels of glucose. Mol. Cell. Biol. 15, 1564–1572.

Runquist, D., Hahn-Hagerdal, B., Radstrom, P., 2010. Comparison of heterologous xylose transporters in recombinant *Saccharomyces cerevisiae*. Biotechnol. Biofuels 3.

Sassner, P., Galbe, M., Zacchi, G., 2008. Techno-economic evaluation of bioethanol production from three different lignocellulosic materials. Biomass Bioenergy 32, 422–430. http://dx.doi.org/10.1016/j.biombioe.2007.10.014.

Sedlak, M., Ho, N.W.Y., 2004. Characterization of the effectiveness of hexose transporters for transporting xylose during glucose and xylose co-fermentation by a recombinant *Saccharomyces* yeast. Yeast 21, 671–684. http://dx.doi.org/10.1002/yea.1060.

Sonnleitnert, B., Kappeli, O., 1986. Growth of *Saccharomyces cerevisiae* is controlled by its limited respiratory capacity: formulation and verification of a hypothesis. Biotechnol. Bioeng. 28, 927–937. http://dx.doi.org/10.1002/bit.260280620.

Tanino, T., Hotta, A., Ito, T., Ishii, J., Yamada, R., Hasunuma, T., Ogino, C., Ohmura, N., Ohshima, T., Kondo, A., 2010. Construction of a xylose-metabolizing yeast by genome integration of xylose isomerase gene and investigation of the effect of xylitol on fermentation. Appl. Microbiol. Biotechnol. 88, 1215–1221. http://dx.doi.org/10.1007/s00253-010-2870-2.

Wingren, A., Galbe, M., Zacchi, G., 2003. Techno-economic evaluation of producing ethanol from softwood: comparison of SSF and SHF and identification of bottlenecks. Biotechnol. Prog. 19, 1109–1117. http://dx.doi.org/10.1021/bp0340180.